ELSEVIER

Journal of Nuclear Materials 257 (1998) 199–205

journal of nuclear materials

Letter to the Editors

Effect of microstructure on the susceptibility of a 533 steel to temper embrittlement

S. Raoul [a,*], B. Marini [a], A. Pineau [b]

[a] CEA- CEREM, Service de Recherches Métallurgiques Appliquées, 91191 Gif/Yvette cedex, France
[b] Centre des Matériaux, Ecole des Mines, UMR CNRS 7633, BP 87, 91003 Evry cedex, France

Received 19 May 1998; accepted 29 June 1998

Abstract

In ferritic steels, brittle fracture usually occurs at low temperature by cleavage. However the segregation of impurities (P, As, Sn etc...) along prior γ grain boundaries can change the brittle fracture mode from transgranular to intergranular. In quenched and tempered steels, this segregation is associated with what is called the temper-embrittlement phenomenon. The main objective of the present study is to investigate the influence of the as-quenched microstructure (lower bainite or martensite) on the susceptibility of a low alloy steel (A533 cl.1) to temper-embrittlement. Dilatometric tests were performed to determine the continous-cooling-transformation (CCT) diagram of the material and to measure the critical cooling rate (V_c) for a martensitic quench. Then subsized Charpy V-notched specimens were given various cooling rates from the austenitization temperature to obtain a wide range of as-quenched microstructures, including martensite and bainite. These specimens were subsequently given a heat treatment to develop temper embrittlement and tested to measure the V-notch fracture toughness at −50°C. The fracture surfaces were examined by SEM. It is shown that martensitic microstructures are more susceptible to intergranular embrittlement than bainitic microstructures. These observed microstructural influences are briefly discussed.

1. Introduction

It is now well established that an important source of scatter in the fracture toughness properties of low alloy steels (A 508, A 533) used in nuclear industry arises from the presence of small areas of low toughness called 'ghost lines'. These local brittle zones which result from the segregation phenomenon associated with ingot solidification have a composition in alloying elements (C, Mn, Ni, Mo) and in impurities (P, S) different from the matrix. The alloying elements control the hardness and the microstructure of these segregated zones which tend to have a martensitic microstructure while the microstructure of the matrix material is bainitic. Moreover these local brittle zones contain increased amounts in impurities such as P, Sn, As which promote intergranular fracture when they are segregated along prior γ grain boundaries [1–4]. In a limited number of studies, it was also shown that in these steels, the susceptibility to intergranular embrittlement was also an increasing function of cooling rate [5,6]. This would suggest that martensitic microstructures resulting from these increased quenching rates are more susceptible to temper-embrittlement. However, to the knowledge of the authors, this suggestion has not been proved. This is why in the present study we have concentrated on the effect of as-quenched microstructures on temper-embrittlement and intergranular fracture. This study was carried out on an A 533 steel with a reasonably homogeneous composition which was submitted to a wide range of cooling rates in order to develop widely different microstructures.

* Corresponding author. Tel.: +33-1 69 08 68 72; fax: +33-1 69 08 71 67; e-mail: raoul@centre.saclay.cea.fr.

0022-3115/98/$ – see front matter
PII: S0022-3115(98)00467-X

2. Experiments, results and discussion

The plate of A 533 cl.1 material used in the present study was investigated within the context of the AIEA-JRQ program. The material composition is given in Table 1. The relatively large amount in P impurity which is well known to promote temper-embrittlement effect has to be noticed. The grain size of the material in the as-received condition was approximately 20 μm.

Various heat treatments as indicated in Fig. 1 were applied to this material. Dilatometric experiments which are described below were carried out to determine the continous-cooling-transformation (CCT) diagram. As indicated schematically in Fig. 1, subsized Charpy V-notched specimens ($16 \times 3 \times 2.2$ mm^3) were submitted after austenitization and phase transformation to a tempering heat treatment followed by a step-cooling heat treatment which is known to promote temper-embrittlement effect.

2.1. Dilatometric measurements

The austenitization treatment and the various cooling rates ($\dot{\theta}$) were carried out with an Adamel-Lhomargy high speed dilatometer (DT1000). This computer controlled equipment allowed us to investigate the effect of cooling rate from 1100°C over the range between 0.02°C/s and 50°C/s. The dilatometric specimens ($16 \times 3 \times 2.2$ mm^3) were cut in the plate with the length parallel to the rolling direction. All these dilatometric tests were performed under a helium atmosphere in order to avoid any decarburization. The heating rate from room temperature up to 1100°C was kept constant and equal to 10°C/s for all the specimens, while the austenitization time was $\frac{1}{2}$ h. This resulted in a prior austenite grain size of approximately 150 μm.

The CCT diagram obtained with this equipment is shown in Fig. 2 where it is observed in particular that the bainitic transformation occurs over a wide range of low cooling rates.

Table 1
Chemical composition (wt %)

C	Mn	Si	Cr	Ni	Mo	S	P
0.2	1.38	0.25	0.15	0.83	0.49	0.009	0.017
Cu	Al	As	Sn	Sb	Ti	Nb	V
0.14	0.024	0.0017	<0.0005	0.0006	0.005	0.006	0.005

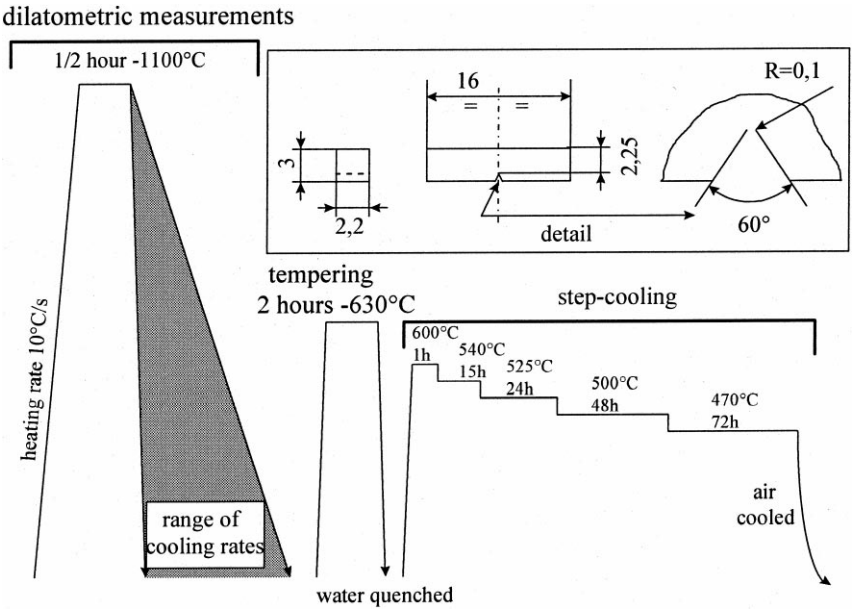

Fig. 1. Heat treatments performed on the JRQ steel and dimensions of the subsized Charpy V-notched specimens.

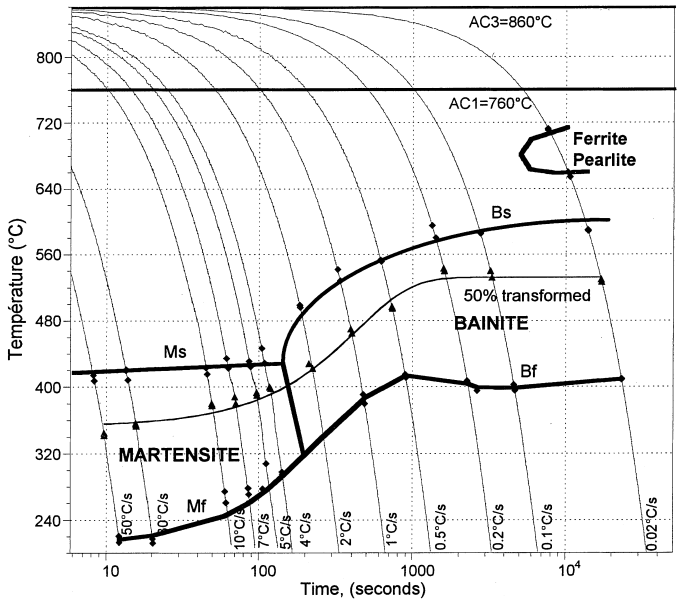

Fig. 2. CCT diagram for the JRQ steel after austenitization $\frac{1}{2}$ h at 1100°C.

In this figure, it is noticed that the critical cooling rate (V_c) to obtain martensite is about 3°C/s. Typical bainitic and martensitic microstructures obtained with different cooling rates located on both sides of V_c are shown in Fig. 3.

2.2. Temper-embrittlement

All the specimens were first tempered at 630°C for 2 h. For that purpose, the specimens were vacuum encapsulated in quartz tubes. These capsules were quenched in a cold water bath after the end of the tempering heat treatment. Then, the specimens were given the step-cooling heat treatment as indicated in Fig. 1. After these heat treatments, light optical examinations were performed using Nital 2% etching. Typical micrographs are shown in Fig. 4 where it is observed that the prior austenite grain boundaries cannot be evidenced when the material has been submitted to a martensitic quench while the grain boundaries are easily revealed in the bainitic microstructure.

The Vickers hardness (30 kg) of the tempered specimens was measured and compared to that of the as-quenched microstructures. The results shown in Fig. 5 clearly indicate that only martensitic microstructures exhibit a pronounced softening effect associated with the tempering heat treatment.

2.3. Notch fracture toughness

The dilatometric specimens were V-notched (depth = 0.75 mm; $V_{angle} = 60°$; notch tip radius = 0.1

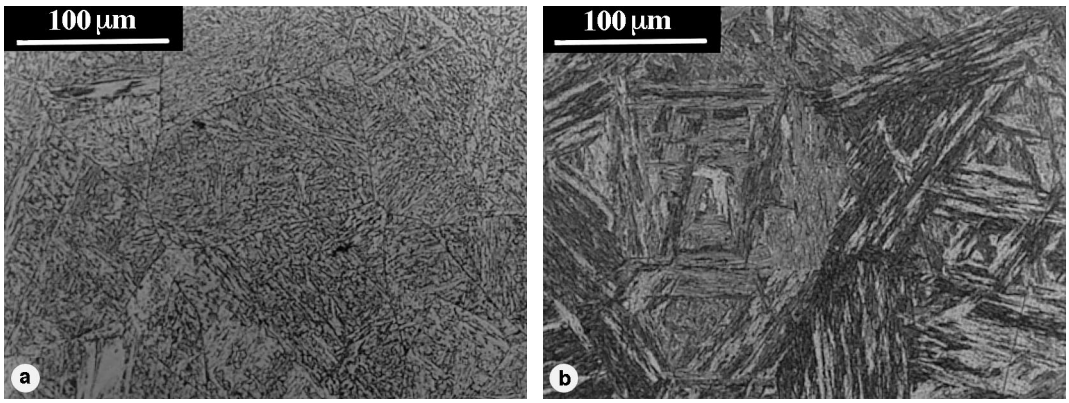

Fig. 3. Light-optical micrographs of the JRQ steel after cooling at (a) 0.5°C/s (bainite) and (b) 10°C/s (martensite).

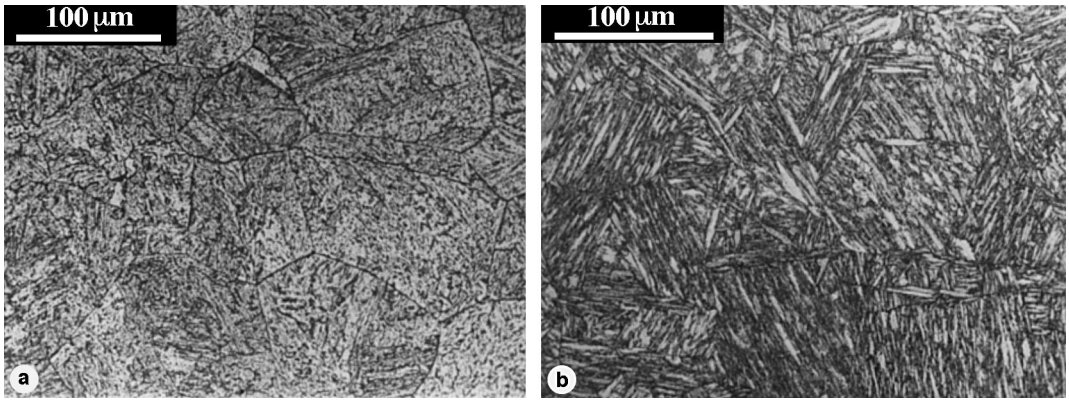

Fig. 4. Light-optical micrographs of the JRQ steel after tempering and step-cooling treatment at (a) 0.5°C/s (bainite) and (b) 10°C/s (tempered martensite).

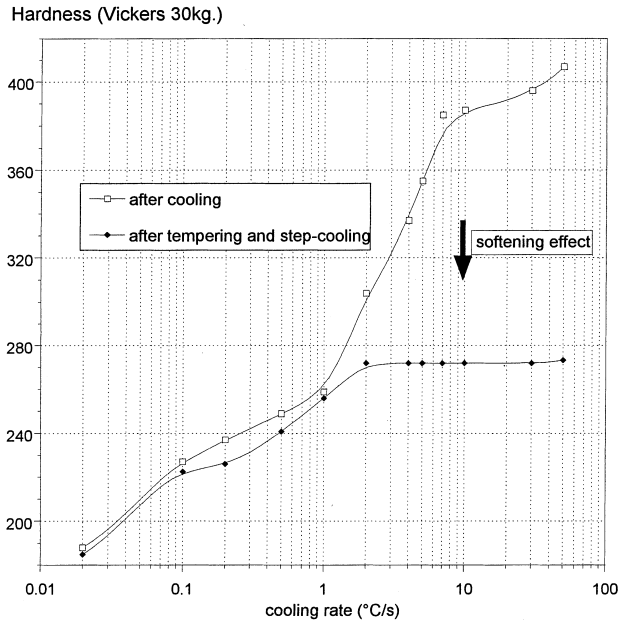

Fig. 5. Vickers hardness (30 kg) after tempering and step-cooling vs. cooling rate.

mm) to produce susbsized V-notched impact specimens (Fig. 1). These notched specimens were tested at −50°C which is a temperature in the brittle range at the onset of the brittle–ductile transition. The notch fracture toughness (K_{CV}) was measured. SEM observations were made on the fracture surfaces to determine the fraction area of intergranular (I_f) and cleavage modes. Fig. 6 shows these results which were fitted with the following expression:

$$K_{CV}\left(\dot{\theta}\right), I_f\left(\dot{\theta}\right) = \alpha + \beta \tanh\left(\left(\dot{\theta} - \dot{\theta}_0\right)/\delta\right), \quad (1)$$

where the values of the four parameters, α, β, $\dot{\theta}_0$ and δ are given in Table 2.

In Fig. 6, it is noted that in spite of the scatter, there is a transition both in the notch fracture toughness and in the fracture mode. This transition corresponds to a cooling rate ($\cong 1°C/s$) which is very similar to the critical cooling rate, V_c, determined previously for martensitic quenching microstructure. This clearly shows that in this material, martensite is much more susceptible to intergranular temper-embrittlement effect than bainite.

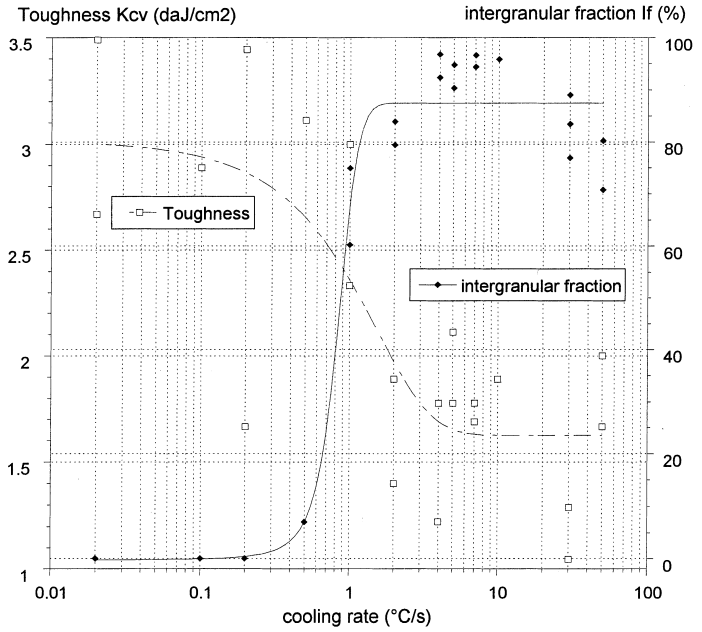

Fig. 6. Toughness and intergranular fraction area vs. cooling rate; tests at −50°C.

Table 2
Fitted parameters for K_{cv} and I_f with Eq. (1)

	α	β	$\dot{\theta}_0$ (°C/s)	δ
K_{CV}	3.65	2.03	−0.755	−2.33
I_f	43.47	44	0.83	0.28

2.4. Fracture surface examination

Typical fracture surfaces corresponding to 100% cleavage associated with bainite produced by a low cooling rate (0.2°C/s) and to 100% intergranular obtained with martensite formed at a higher cooling rate (4°C/s) are shown in Fig. 7. These observations are similar to those reported by other authors [5–7]. But here, it is clearly shown that this modification in fracture mode with cooling rate is associated with a change in microstructure from bainite ($\dot{\theta} \cong 3$°C/s) to martensite ($\dot{\theta} \geqslant 3$°C/s). Here it should be indicated that this transition in fracture modes may be slightly different in other heats of the same family, depending on small compositional modifications or austenitizing conditions. Larger

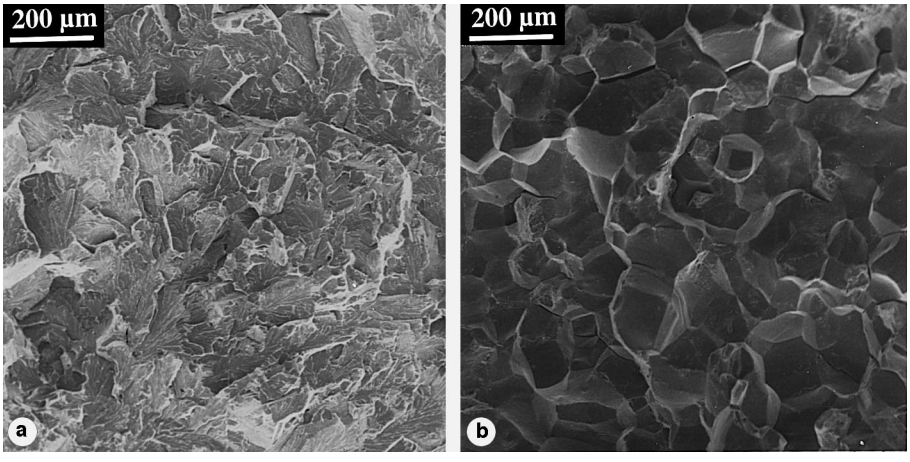

Fig. 7. SEM fractographs of V-notched-Charpy fractured specimens tested at −50°C for two different tempered-step-cooled microstructures: (a) 0.2°C/s (100% cleavage); and (b) 4°C/s (100% intergranular).

variations in the critical cooling rate (V_c) are expected locally in the ghost lines of strongly segregated materials since the examination of the local composition indicates significant variations [8].

2.5. Fracture surface analysis

Auger electron spectroscopy (AES) studies of grain boundary segregation in steels have been made over the last past 20 years in order to identify the trace elements responsible for temper-embrittlement [9,10]. It has been shown that phosphorus is mainly responsible for temper-embrittlement.

In the present study, AES analyses were made on intergranular fracture surfaces obtained on the material cooled at 4°C/s, tempered and step-cooled. Double notched specimens with a cross section of 3×1 mm^2 were used. These specimens were cooled in the AES chamber to approximately −50°C before being broken by impact bending inside the analysis chamber (vessel back pressure less than 10^{-8} Pa). Fracture surfaces were examined using secondary electron images. AES analyses were made on many (12) facets. A cylindrical mirror analyzer (OPC 105-RIBER) was used with a coaxial electron gun operating at 2.5 keV primary beam energy with a 30° incidence to the sample normal onto a 30 μm diameter area. Conventional derivative spectra similar to that shown in Fig. 8 were obtained with a 3 V modulation voltage applied to the analyzer. Taking into account the measurements errors, no difference was observed between the different facets in a specimen. As shown in Fig. 8, the segregation of phosphorus and molybdenum was clearly observed. Manganese, sulfur and arsenic were not detected in spite of their bulk content. The segregation coverage 2ϕ was defined as the surface fraction of the homogeneous alloy covered by segregated atoms (P and Mo). Assuming an equal partition of elements between the fracture surfaces, we finally evaluate the mean phosphorus coverage as $2\phi \cong 50\%$ and the molybdenum coverage $2\phi \cong 13\%$.

Further observations of the fracture surfaces were made using field emission scanning electron microscopy observations of intergranular facets. These observations showed numerous submicronic particles along grain boundaries as shown in Fig. 9. TEM analysis of these particles using carbon replicas showed that they correspond to Mo_2C carbides.

Further studies are underway to understand in more detail these observations. It is suggested that martensitic microstructures formed within the prior γ grain contain essentially low angle grain boundaries between the various packets while in the bainitic microstructure a larger amount of large angle grain boundaries may be found. This might explain at least qualitatively our observations since in the martensitic microstructures the impurities are expected to essentially segregate along the prior austenite grain boundaries, while in the bainitic microstructure the density of sinks for impurity segregation will be larger due to the presence of large angle grain boundaries and therefore the intensity of impurity segregation will be lower. EBSD observations will be made shortly since it has been recently shown that this technique may be appropriate to determine the orientation between the packets in bainitic and martensitic steels [11].

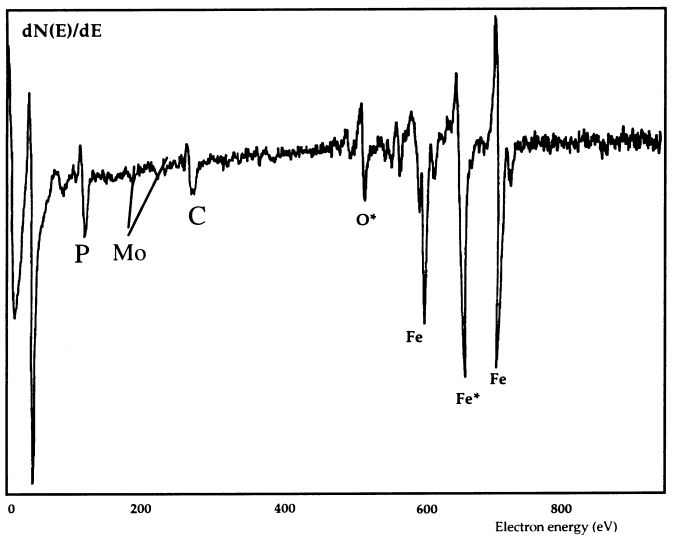

Fig. 8. Auger spectrum from an intergranular fracture area of the embrittled microstructure.

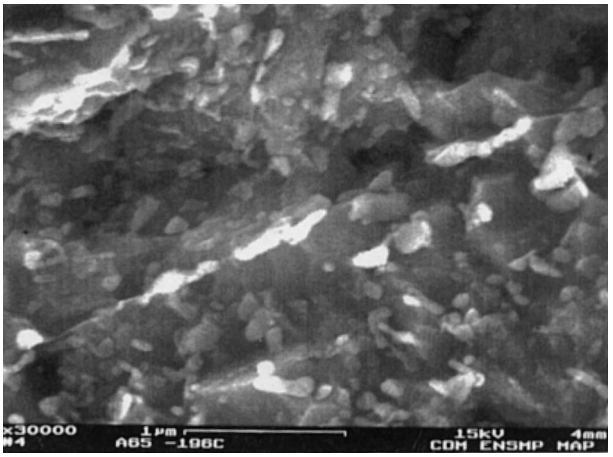

Fig. 9. High resolution SEM image of an intergranular fracture showing the distribution of small molybdenum carbides.

3. Conclusions

It can be concluded from the present study that the tempered martensitic microstructures are more susceptible to intergranular embrittlement than the bainitic ones for a low alloy steel containing a significant quantity of phosphorus. For the intergranular embrittlement, the phosphorus segregation is mainly responsable for the embrittlement and molybdenum plays perhaps an important role via the presence of colonies of submicronic carbides on intergranular facets. One can make the assumption that the bainitic phase transformation drags the phosphorus atoms in the high angle interlaths boundaries, and then phosphorus is less susceptible to diffuse to prior γ grain boundaries. On the contrary, the high coincidence lath and packet boundaries in martensitic microstructures let the phosphorus free in the matrix. This impurity can then segregate to prior γ grain boundaries. A second explanation for these results may lie upon the tempering treatment effect on carbide precipitation in the martensitic microstructure which is susceptible to drag phosphorus to defects sinks like the prior γ grain boundaries.

Acknowledgements

We are pleased to thank the friendly cooperation of Dr J.C. Brachet and A. Castaing from SRMA-CEA/Saclay for their experimental contribution and valuable discussions on the dilatometric measurements. The Auger electron analysis were performed at the Centre d'Etudes de Chimie Métallurgique from the CNRS of Vitry/Seine. Dr G. Lorang from this Institute is greatly acknowledged.

References

[1] M. Guttmann, P. Dumoulin, M. Wayman, Metall. Trans. 13A (1982) 1693.
[2] J.R. Rice, J.S. Wang, Mater. Sci. Eng. A107 (1989) 23.
[3] S.G. Druce, G. Gage, G. Jordan, Acta Metall. 34 (4) (1986) 641.
[4] D.Y. Lee, E.V. Barrera, J.P. Stark, H.L. Marcus, Metall. Trans. 15A (1984) 1415.
[5] D. Tigges, Nocivité des défauts sous revêtement des cuves de réacteurs à eau sous pression, thèse Ecole des Mines de Paris, Mars 1995.
[6] E. Kantidis, Rupture fragile intergranulaire d'un acier faiblement allié, approches globale et locale, thèse Ecole des Mines de Paris, Juin 1993.
[7] O.M.L. Yahya, F. Borit, R. Piques, A. Pineau, Statistical modelling of intergranular brittle fracture in a low alloy steel, submitted to Fatigue Fract. Eng. Materi. Struct.
[8] P. Le Bec, D. Renaud, J.C. Van Duysen, Caractérisation structurale et mécanique de produits représentatifs de zones ségrégées (veines sombres) d'aciers de cuves REP, EDF report, Département Etude des Matériaux, 1995.
[9] B.C. Edwards, H.E. Bishop, J.C. Rivière, B.L. Eyre, Acta Metall. 24 (1976) 957.
[10] G. Thauvin, G. Lorang, C. Leymonie, Metall. Trans. 23A (1992) 2243.
[11] E. Bouyne, H.M. Flower, T.C. Lindley, A. Pineau, Use of EBSD technique to examine microstructure and cracking in a bainitic steel, submitted for publication to Scri. Mater.